Study of ADI(After Develop Inspection) Using Electron Beam

Misako Saito[a], Teruyuki Hayashi [a], Kaoru Fujihara [a], Kazuha Saito [a],
Joseph Lin [b], Ryotaro Midorikawa [a]
[a] Tokyo Electron Ltd., 650 Mitsuzawa, Hosaka-cho, Nirasaki City, Yamanashi, Japan;
[b] Hermes Microvision Inc.,5F,No.18,Creation Road 1 Science Park,Hsin-Chu,300,Taiwan,R.O.C.

ABSTRACT

In this paper, we established a method to detect defects with a size of 40nm, which is required in the machine to inspect defects on the photo resist of hp65nm generation. First of all, we clarified the mechanism of nuisance generation by electron beam and established a method to control nuisances. Next, we examined the inspection conditions required for detection of minute defects. As a result, the relation between the landing energy, brightness, or contrast and the defect detection ratio were clarified. We successfully detected minute defects of 40nm in the inspection based on a strategies obtained from these examination results to confirm that we established a method to detect minute defects. In addition, we compared defects on photo resist in electron beam inspection and electric defects in the wiring resistance measurement. As a result, the defect distribution on photo resist was found identical to the electric defect distribution. Thus, we proved that the defect inspection on photo resist using electron beam was detecting the killer defects. Therefore, we showed that the resist defect inspection using electron beam is effective for the 65nm generation.

Keywords: inspection, photo resist, electron beam

1. INTRODUCTION

According to the ITRS, the defect size that must be controlled is 40nm for the generation with technology node of hp65nm. In consideration of that, it is thought that defect inspection machines of hp65nm generation or later may have difficulties in inspection if they use the conventional optical systems that are mainly used at present. Therefore, a study is being made into defect inspections using electron beam which have superior resolution. However, there are only a few examples in which defect inspection on photo resist using electron beam is examined. It is not known whether the electron beam is effective or not for defects on photo resist.

Defect inspection systems using electron beam have begun to be introduced to the processes other than that for photo resist. Their efficacy have been reported with regard to detection performance of voltage contrast and minute defects which is a feature of electron beam inspections [1,2,3]. Nevertheless, in the photo resist process, the majority of defects are shape defects, excessive particles, or others found in photo resist itself. It is impossible to detect these defects by voltage contrast. Also, there are no examples verified whether it is possible to detect minute defects smaller than 40nm on photo resist, or whether defects detected by electron beams are so-called killer defects. The detection performance of electron beam systems has been called into question.

Therefore, we decided to prove the efficacy of the defect inspection using electron beam for 65nm and subsequent generations by grasping the characteristics of the electron beam inspection machine and developing the method to detect minute defects and the method to reduce nuisance.

2. CLARIFICATION OF NUISANCE GENERATION MECHANISM AND DEVELOPMENT OF METHOD TO REDUCE THEM

It is essential for defect inspection machines to have an ability to detect only a small number of nuisances as well as an ability to detect defects. Because the principle of electron beam system is different from that of the optical system, nuisance peculiar to the electron beam system, which are not caused by the optical system, may be generated. Therefore, we first checked whether any nuisances peculiarly caused by electron beam are generated, and then clarified the nuisance generation mechanism and developed a method to reduce the nuisance.

Metrology, Inspection, and Process Control for Microlithography XX, edited by Chas N. Archie, Proc. of SPIE Vol. 6152, 615248, (2006) · 0277-786X/06/$15 doi: 10.1117/12.656090

2.1 Nuisance generation by electron beam

We prepared sample of 110nm 1:1 L/S of photo resist/BARC/Poly-Si, and we made programmed defects of open shape in it. We took the scanning electron microscope (SEM) images for various voltages as shown Fig.1. At the landing energies of 300eV and 1500eV, the open shaped programmed defects could be observed clearly. At the landing energy of 1000eV, however, we saw a lot of black spots in the space in addition to open defect. These black spots may be highly possibly detected as nuisance. Since they depend on the landing energy, they can be considered to be nuisance peculiar to the electron beam. We determined for the cause of these nuisances.

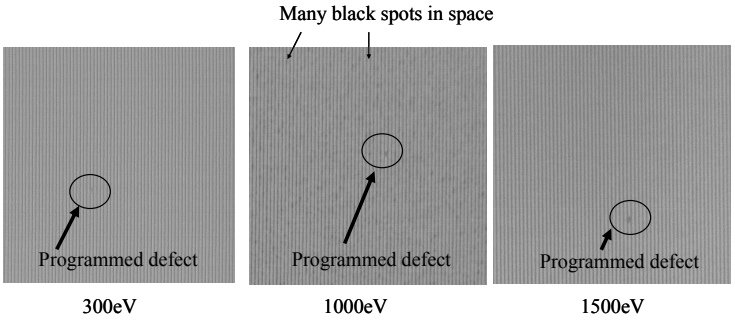

Fig. 1 Difference of SEM images depends on landing energy.

First, we removed the photo resist and BARC and observed the Poly-Si morphology by SEM and measured surface roughness (Ra) using atomic force microscope (AFM). As shown in Fig. 2, Poly-Si surface morphology is large. We coating BARC and photo resist on Poly-Si having a smaller morphology to form a pattern of L/S and obtained the SEM image by electron beam. Fig. 3 illustrates the results. No black spots were observed when the Poly-Si surface morphology was small. From these results, we can judge that the black spots observed at the landing energy of 1000eV represent the Poly-Si morphology.

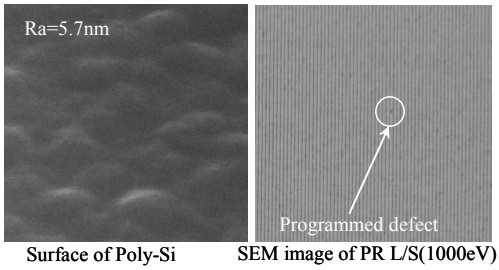

Fig. 2 Poly-Si surface morphology of the sample with black spots.

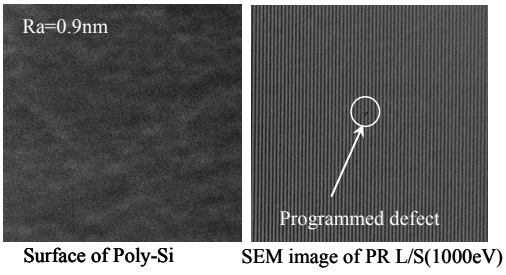

Fig. 3 The SEM image of PR pattern on the smooth Poly-Si surface.

2.2 Clarification of nuisance generation mechanism

To evaluate the black spot generation numerically, we checked the dependency of the nuisance on the landing energy in number. Fig.4 shows relationship between landing energy and nuisance detection quantity. In low landing energy of

300eV or below and of a high landing energy of 1500eV, no nuisance was detected. At 800eV, many nuisances were detected. In order to find out the mechanism of black spot generation at a specific landing energy, we calculated the penetration depth of primary electrons to the specimen using Monte Carlo simulation. Fig. 5 shows relationship between landing energy and penetration depth of primary electron. At 300eV, primary electrons reach inside of BARC only. At 800eV, on the other hand, many electrons reach the Poly-Si surface. Primary electrons reflected by the Poly-Si surface generate secondary electrons near the surface of the BARC. It is considered that, when the secondary electrons generated near the surface of BARC reach the detector, the morphology information on the Poly-Si surface is detected. Because BARC has a low density, primary electrons easily reach the Poly-Si surface and reflected electrons easily reach the surface of the BARC, which seems to help generation of black spots. When the landing energy is further raised, many primary electrons reach the inside of Poly-Si and the smaller numbers of electrons are reflected at the interface. This coincides with the phenomenon that no black spot is observed at a landing energy of 1300eV or higher. Based on the results above, we confirmed the correlation of the nuisance detection quantity and Monte Carlo simulation and we could clarify the black spot generation mechanism. We verified that it is possible to select the landing energy level by Monte Carlo simulation as a method to reduce nuisance.

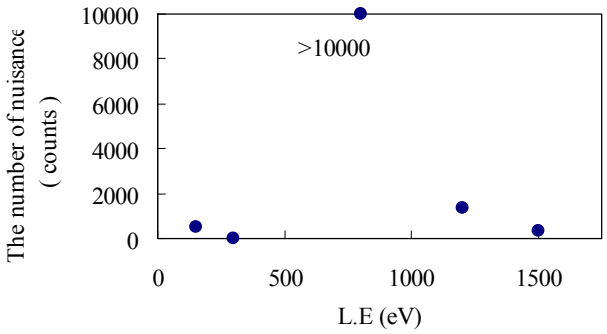

Fig. 4 The relationship between L.E and nuisance detection quantity

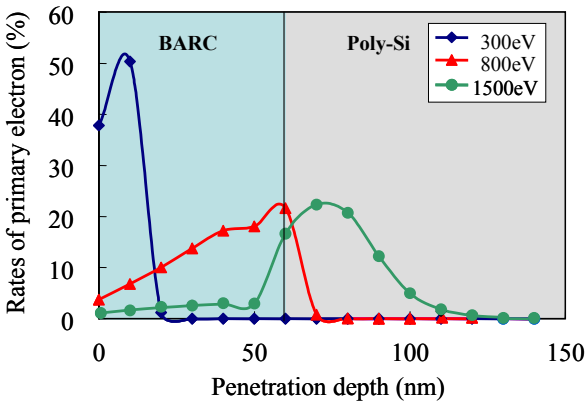

Fig. 5 The relationship between L.E and calculated penetration depth of primary electron by Monte Carlo simulation.

3. ESTABLISH A METHOD TO DETECT DEFECTS OF 40nm OR LESS

In observation of specimens by electron beam, their images obtained are totally different depending on the landing energy. A low landing energy is effective to obtain the surface information, and internal information can be obtained at a high landing energy. In addition, it is known that the resolution is improved but the edge effect increases at a high landing energy. In case of SEM, convex and concave sections are in monochrome images and the specimen appears differently depending on the contrast and brightness. Therefore, we clarified how these parameters influence the detection of minute defects of 40nm on photo resist and established a method to detect minute defects.

3.1 Landing energy dependency

We evaluated the landing energy dependency in detection of defects on photo resist. We conducted a defect inspection for the programmed defects as shown in Fig. 6 and calculated the programmed defect detection ratio with a constant threshold. Fig. 7 shows landing energy dependency of capture rate of programmed defect. It is understood that the defects are detected at a high ratio under the condition with a high landing energy. Generally, it is known that the resolution is improved at a higher landing energy. From the results above, we found that the high landing energy which enables a high resolution is appropriate in order to improve the defect detection ratio on photo resist.

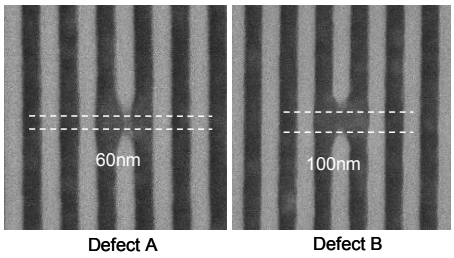

Fig. 6 The SEM pictures of programmed defects in 110nm L/S of photo resist.

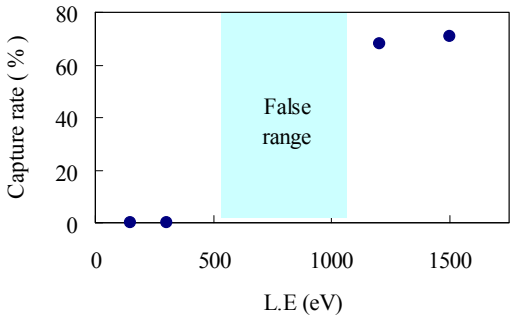

Fig. 7 The landing energy dependency of capture rate of programmed defects.

3.2 Contrast and brightness dependency

Next, we checked how the defect detection ratio depends on contrast gain and brightness gain. We obtained the SEM images of programmed defects under different contrast and brightness gains and, as shown in Fig. 8, analyzed the gray level of the defect region and the space region. Fig. 9 shows the calculation results of the gray level difference between the defect region and the space region for different contrast condition under the fixed brightness. We can see that the gray level difference becomes larger as the contrast becomes higher. Since the defect detection depends on the gray level difference, a higher contrast may improve the defect detection ratio. Similarly, we checked the influence of the brightness. Fig. 10 shows brightness dependency of gray level difference between defect region and space region. The absolute value of the gray level as a whole is changed by brightness change. However no change is observed in the gray level difference between the defect region and the space region. Therefore, it can be considered that the brightness does not largely influence the defect detection ratio. Based on the above, we concluded that the contrast influences the defect defection ratio, but the brightness does not influence it.

Here, we actually compared the detection ratio of the programmed defects under two conditions with different contrasts. We inspected the photo resist/BARC/P-Sub specimens of 110nm 1:1 L/S for an area of 250μm * 300μm having programmed defects and compared their defect detection ratio. Fig.11 shows the SEM image of programmed defects for inspection. Fig.12 shows defect detection ratio on two contrast condition. As expected, it was confirmed that the defect detection ratio was higher for the condition with a higher contrast gain.

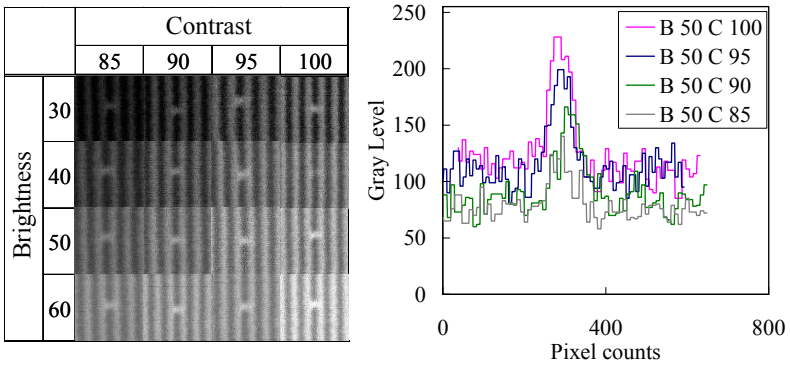

Fig. 8 The SEM images and gray level value of programmed defects depends on contrast/brightness gain.

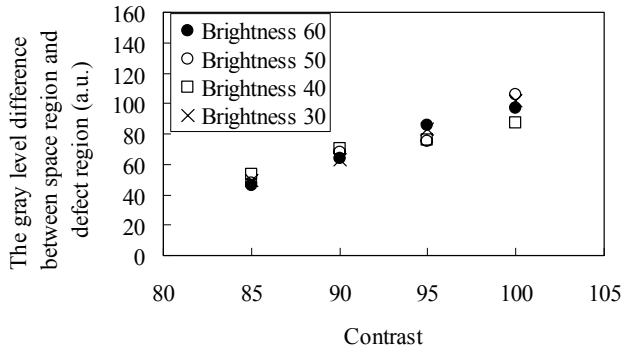

Fig.9 The contrast dependency of gray level difference between the defect region and space region.

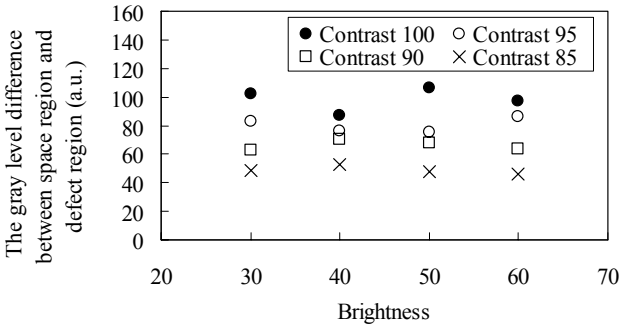

Fig.10 The brightness dependency of gray level difference between defect region and space region.

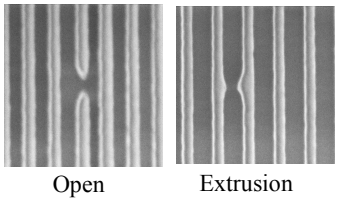

Fig.11 The SEM images of programmed defect of photo resist.

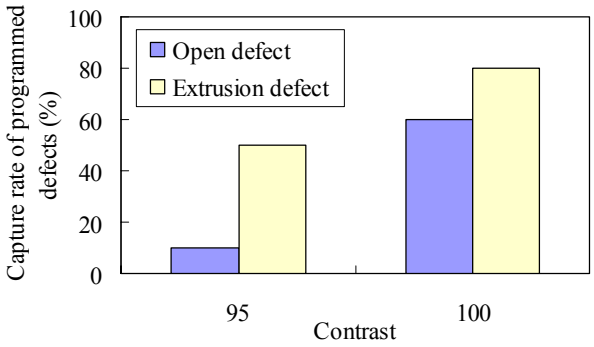

Fig.12 The relationship between contrast gain and capture rate of programmed defect.

3.3 Detection of 40nm or smaller defects

From the examination results so far, it is understood that selection of landing energy for a fewer nuisance by Monte Carlo simulation, selection of high landing energy to obtain a high resolution, and selection of a contract that facilitates the defect detection improve the detection ratio of minute defects. Under these conditions, we conducted an inspection for minute defects of 40nm or less. The samples were programmed defects on 110nm 1:1 L/S, the shape of bridge, open, and extrusion defects were prepared. They were gradually different in their sizes between 200 and 20nm. Fig. 13 illustrates the inspection results. The circled defects could be detected and those in triangles could not be detected under these conditions. It is learned that defects below 40nm were detected under the inspection conditions set here. Thus, we established a method to detect defects with sizes of 40nm or less.

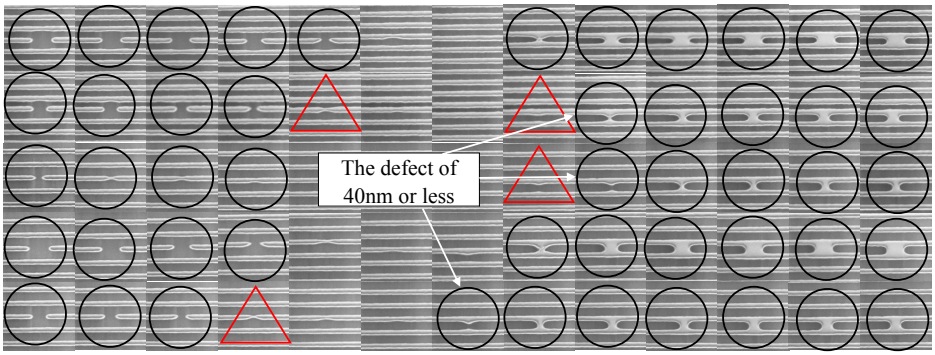

Fig.13 The inspection result of 193nm L/S resist bridging and open defects by the optimized condition.

4. CORRELATION BETWEEN PHOTO RESIST DEFECT GENERATED IN DEVICE MANUFACTURING PROCESS AND ELECTRIC CHARACTERISTICS

Next, we evaluated whether killer defects generated in the device manufacturing process can be detected using comb-shaped TEG. Fig.14 shows the procedure to manufacture samples. After forming Th-ox and Poly-Si films on bare-silicon, we applied BARC and photo resist to it and prepared two pattern wafers having comb shapes. We left one as it was with photo resist and etched Poly-Si film on the other to prepare a Poly-Si comb pattern. We inspected photo resist and Poly-Si comb pattern for defects and measured their leakage current. Fig.15-a shows the defect inspection results on photo resist. The figure shows that defects were concentrated at the center of the left end of the die. Fig.15-b shows the results of defect observation using review SEM. The detected defects were bridges having about a half the width of the line. Next, Fig.16-a shows the Poly-Si defect inspection results. As in the case of photo resist defects, the defects were concentrated at the center on the left end of the die. Fig.16-b shows SEM image by review SEM. And Fig.16-c shows the results of cross-sectional observation by FIB-SEM for this bridge defect region. It is understood that the lines are connected at the bottom. Further, Fig. 17 shows the results of leakage current

measurement for this sample. As in the cases of the photo resist and Poly-Si, there were many short failures around the center on the left side of the die. Based on these results, it is found that killer defects on photo resist generated in the device manufacturing process can be detected with higher sensitivity by the electron beam inspection.

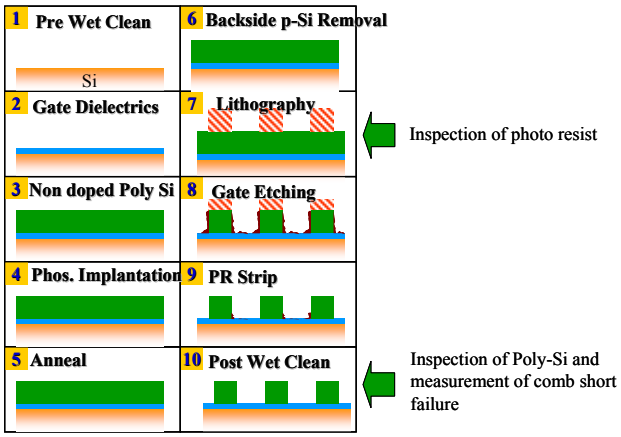

Fig.14 The schematic illustration of test wafer processing.

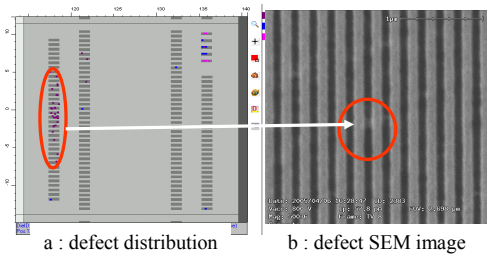

a : defect distribution b : defect SEM image

Fig. 15 The defect distribution in the chip and the SEM image of detected defect of the photo resist pattern.

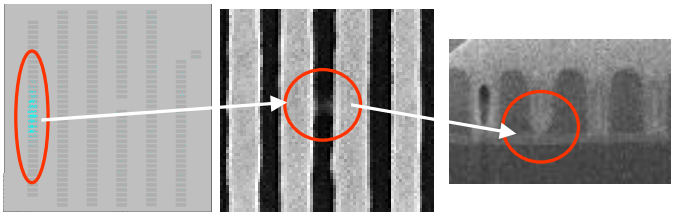

a : defect distribution b : defect SEM image c : defect cross-section

Fig.16 The defect distribution in the chip and cross-section image of defect by FIB-SEM of poly-Si pattern.

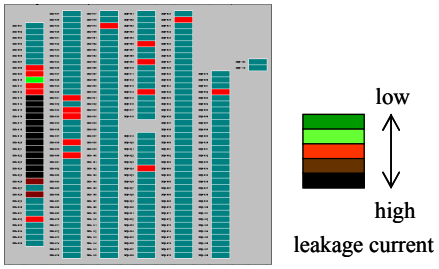

Fig.17 The poly-Si comb short failure distribution in the chip.

5. CONCLUSION

We established a method to detect 40nm defects required in the machine of hp65nm generation to inspect defects on the photo resist. First, we confirmed that the morphology of under layer is recognized as nuisance in the defect inspection using electron beam and, by Monte Carlo simulation analysis, clarified the generation mechanism of nuisance. In addition, we clarified by Monte Carlo simulation that the nuisance can be controlled. Next, we clarified the relation between the landing energy, brightness, or contrast and the defect detection ratio in the minute defect detection. We conducted an inspection under these conditions and successfully detected minute defects of 40nm.
We further prepared comb-shaped patterns and compared the photo resist defect inspections and comb short failures. As a result, the defect detection distribution on photo resist was identical to the comb short failure distribution. We found that we can detect killer defects with high sensitivity by the photo resist defect inspection using electron beam. Therefore, it is considered that the photo resist defect inspection using electron beam is effective for the 65nm generation.

ACKNOWLEDGEMENT

The authors would like to thank Professor Kaoru Ohya, University of Tokushima for calculation of Monte Carlo simulation.

REFERENCES

1. Jack Jau, et al, "A Novel Method for In-line process Monitoring by Measuring Gray Level Values of SEM images", Proceedings of ISSM, September 2005,pp143-146.
2. X. Liu, et al, "Low energy large scan field electron beam column for wafer inspection", Journal of Vacuum Science& Technology B, Volume 22, Number 6, pp. 3534-3538.
3. Samantha L.Doan, "Expanding the Role of E-beam Inspection in Sub-130nm Flash Memory Development", Proceeding of ISSM, September 2004,pp464-467.